

Comprehensive Competition Mechanism in Palmprint Recognition

Ziyuan Yang[✉], Huijie Huangfu[✉], Lu Leng[✉], Member, IEEE, Bob Zhang[✉], Senior Member, IEEE,
Andrew Beng Jin Teoh[✉], Senior Member, IEEE, and Yi Zhang[✉], Senior Member, IEEE

Abstract—Palmprint has gained popularity as a biometric modality and has recently attracted significant research interest. The competition-based method is the prevailing approach for hand-crafted palmprint recognition, thanks to its powerful discriminative ability to identify distinctive features. However, the competition mechanism possesses vast untapped advantages that have yet to be fully explored. In this paper, we reformulate the traditional competition mechanism and propose a Comprehensive Competition Network (CCNet). The traditional competition mechanism focuses solely on selecting the winner of different channels without considering the spatial information of the features. Our approach considers the spatial competition relationships between features while utilizing channel competition features to extract a more comprehensive set of competitive features. Moreover, existing methods for palmprint recognition typically focus on first-order texture features without utilizing the higher-order texture feature information. Our approach integrates the competition process with multi-order texture features to overcome this limitation. CCNet incorporates spatial and channel competition mechanisms into multi-order texture features to enhance recognition accuracy, enabling it to capture and utilize palmprint information in an end-to-end manner efficiently. Extensive experimental results have shown that CCNet can achieve remarkable performance on four public datasets, showing that CCNet is a promising approach for palmprint recognition that can achieve state-of-the-art performance. Related codes will be released at <https://github.com/Zi-YuanYang/CCNet>.

Index Terms—Palmprint recognition, comprehensive competition mechanism, deep learning, biometric recognition, texture features.

Manuscript received 1 June 2023; revised 11 August 2023; accepted 11 August 2023. Date of publication 17 August 2023; date of current version 25 August 2023. This work was supported in part by the National Natural Science Foundation of China under Grant 62271335 and Grant 61866028, in part by the Sichuan Science and Technology Program under Grant 2021JDJQ0024, in part by the Sichuan University “From 0 to 1” Innovative Research Program under Grant 2022SCUH0016, in part by the National Research Foundation of Korea (NRF) under Grant NRF-2022R1A2C1010710, and in part by the Technology Innovation Guidance Program Project of Jiangxi Province (Special Project of Technology Cooperation) under Grant 20212BDH81003. The associate editor coordinating the review of this manuscript and approving it for publication was Prof. Walter J. Scheirer. (*Corresponding author*: Yi Zhang.)

Ziyuan Yang and Huijie Huangfu are with the College of Computer Science, Sichuan University, Chengdu 610065, China (e-mail: cziyuanyang@gmail.com; huangfu@stu.scu.edu.cn).

Lu Leng is with the School of Software, Nanchang Hangkong University, Nanchang 330063, China (e-mail: leng@nchu.edu.cn).

Bob Zhang is with the Pattern Analysis and Machine Intelligence Group, Department of Computer and Information Science, University of Macau, Taipa, Macau, China (e-mail: bobzhang@um.edu.mo).

Andrew Beng Jin Teoh is with the School of Electrical and Electronic Engineering, College of Engineering, Yonsei University, Seoul 03722, Republic of Korea (e-mail: bjteoh@yonsei.ac.kr).

Yi Zhang is with the School of Cyber Science and Engineering, Sichuan University, Chengdu 610065, China (e-mail: yzhang@scu.edu.cn).

Digital Object Identifier 10.1109/TIFS.2023.3306104

I. INTRODUCTION

PALMPrint recognition has received significant attention recently due to its potential for various applications [1]. For example, the unique features of the palm, including wrinkles, ridges, and minutiae, make it a distinct biometric trait that can be used for precise identity management. In addition, palmprint recognition is a viable option for biometric recognition systems because it eliminates the risk of potential health hazards that come with contact-based biometric recognition systems. This is especially relevant during times of epidemics. Hence, palmprint recognition has become a popular research area.

Recently, numerous palmprint recognition methods have been proposed, achieving impressive performances [2]. Many were specifically designed to extract discriminative texture features from palmprint images. Gabor filter is widely recognized as one of the most powerful tools for this task, and many works were designed based on some specific filters [3]. For example, PalmCode [4] attempted to extract texture features by convolving the palmprint image with a 2D Gabor filter along 45°, and the convolved features were coded to increase the matching speed and reduce the storage cost. Inspired by PalmCode, extensive magnitude feature-based palmprint recognition methods were proposed. However, these methods were often sensitive to rotation or dislocation of the palmprint image, which limited their effectiveness in practical applications, especially contactless systems.

Kong et al. [5] proposed Competitive Code (Comp Code), which was the first attempt at embedding the competitive mechanism into palmprint recognition. The basic assumption of the competition mechanism is that the magnitude response is maximal when the directions of the filter and the image’s remarkable textures are identical. Comp Code coded the winner index of different features as the feature. Following the idea of Comp Code, many competition-based methods have been proposed [6], [7], [8]. Although these methods achieve competitive performance due to their powerful representation ability of the texture, the potential of competitive mechanism has yet to be fully explored. Two distinct reasons can be identified: 1). The filter extractor is designed primarily based on prior expert knowledge; 2). Current features only account for 1st-order textures across different channels, without considering spatial information and high-order textures.

To address these problems, we reformulate the competition mechanism and propose a novel Comprehensive Competition Network (CCNet) for palmprint recognition in this paper. Our approach aims to overcome the limitations caused by hand-crafted filter design and fully leverage the benefits of

Gabor filters. To achieve this, we introduce a learnable Gabor filter that can automatically learn the optimal hyperparameters to improve recognition performance. Additionally, we design multiple texture extraction branches to capture multi-scale textures.

Traditional competition mechanism selects the winner to represent all channels, which can only identify ‘which’ orientation is best. However, it misses spatial information, which is crucial in determining ‘where’ the best response is located in each feature channel. Unlike the traditional competition-based approach, CCNet extends the competition mechanism by considering spatial competition relationships between features. We employ a strategy of pitting channel features against spatial features in head-to-head competitions. Furthermore, since deep learning (DL)-based methods extract informative features by blending channel and spatial information, we prioritize learning discriminative features from channel and spatial information.

Besides this, traditional competition-based methods solely focus on low-order (first or second-order) texture characteristics. However, higher-order texture features can effectively refine palmprint texture types to enhance the discrimination further. To break through this limitation, CCNet extracts competition features from multi-order textures, enabling the network to capture various texture information. In summary, CCNet integrates spatial and channel competition relationships and multi-order competition relationships to enhance the competition mechanism. This improved mechanism, dubbed Comprehensive Competition Mechanism (CCM), enables extracting comprehensive palmprint features. The main contributions of this paper can be summarized as follows:

- 1) We reformulate the traditional competition mechanism and extend it to extract comprehensive competition features, including channel, spatial, and multi-order competitive features.
- 2) We propose a novel palmprint recognition network, CCNet, which does not rely on prior knowledge and can search for the most effective hyperparameters while developing texture filters during the training phase.
- 3) The proposed CCNet is validated on four public datasets, which can achieve the best performance on each dataset and even achieve 0% EERs on some datasets. Meanwhile, ablation experiments demonstrate that all proposed components of CCM can improve performance effectively.

The rest of this paper is organized as follows. We briefly review the related works in Section II; Section III elaborates on the proposed methodology; Extensive experiments are designed and shown in Section IV; Finally, we conclude this work and provide the future works in Section V.

II. RELATED WORKS

Recently, palmprint recognition has gained considerable attention in various applications. For example, Fei et al. [9] proposed a spectrum-invariant feature learning approach for cross-spectral palmprint recognition, aiming to extract consistent templates from different spectral palmprint images. Iula et al. [10] proposed a novel 3-D ultrasound palmprint recognition system, which combined several 2-D palmprints to build a 3-D template. In this sub-section, we will briefly

review palmprint recognition methods and competitive-based palmprint recognition methods.

A. Palmprint Recognition Methods

Over the past decades, researchers have proposed a great number of palmprint recognition methods [11]. These methods can be broadly categorized into four groups: subspace-based, statistic-based, coding-based, and DL-based methods [12]. Subspace-based methods aim to project palmprint images or features onto a lower-dimensional subspace. Statistic-based methods typically extract hand-crafted features and then employ statistical techniques to identify individual [13]. Sometimes heterogeneous palmprint features can be jointly used to identify individuals [14].

Coding-based methods aim to extract rich discriminative texture features for precise individual identification. Gabor filter is one of the most powerful texture extractors for palmprint recognition [15]. For example, Binary Orientation Co-occurrence Vector (BOCV) [16] was proposed to extract texture features along different orientations using six Gabor filters. Then the magnitude features were coded to generate binarized templates. Inspired by BOCV, Zhang et al. [17] masked fragile bits in BOCV to extract more robust features, and the method was dubbed E-BOCV. Sun et al. [18] proposed extracting ordinal relationships of three pairs of orthogonal orientations, dubbed as Ordinal Code. In Fusion Code [19], the phase with the largest magnitude was extracted and coded. Some plug-and-play downsampling steps were proposed for coding-based methods, such as Extreme Down-sampling Method (EDM) [20]. Recently, Yang et al. [21] proposed 2nd-order Texture Co-occurrence Code (2TCC) by using the 2nd-order texture feature in palmprint recognition and further proposed Multiple-order Texture Co-occurrence Code (MTCC) to combine multiple-order texture features. However, these methods are all based on manually designed texture extractors, and the magnitude feature-based templates are sensitive to illumination change.

Encouraged by the tremendous success of deep learning in vision tasks, researchers are enthusiastic about incorporating DL methods into palmprint recognition. For example, Chai et al. [22] used a convolutional neural network (CNN) and combined the soft biometric information to improve performance. Genovese et al. [23] proposed an unsupervised palmprint recognition method PalmNet, which combined different feature extraction methods, including CNNs, Gabor filters, and principal component analysis. Zhong and Zhu [24] proposed centralized large-margin cosine loss and achieved satisfactory performance. Zhang et al. [25] proposed a deep hashing palm vein network (DHPN) in palm vein recognition, which can be considered as an extension of deep hashing network [26]. Inspired by DHPN, Wu et al. [27] combined DHPN with the spatial transformer modules, resulting in a remarkable performance. Dong et al. [28] introduced cancellable technology into the deep palmprint recognition method and proposed a biometric security recognition framework. Besides this, a co-learning framework was proposed to achieve cross palmprint and palm vein recognition [29]. These magnitude response-based methods have achieved satisfactory performance but are highly sensitive to feature changes, severely jeopardizing their robustness.

B. Competitive-Based Palmprint Recognition Methods

Researchers have attempted to extract competition features to address the limitations of magnitude response-based methods such as PalmCode [4]. Specifically, the magnitude responses along different orientations are compared, and competition results are extracted and coded as the features [5]. Jia et al. [6] used the same competition and coding rules but a new texture extractor, dubbed as Robust Line Orientation Code (RLOC). Half-Orientation Code (HOC) [30] is another work based on the same competition mechanism but half-Gabor filters. Besides this, some researchers focused on extending the competition mechanism by proposing distinct coding rules. For example, Fei et al. [7] presented a Double Orientation Code (DOC), which selected the top-2 winners as the representation of each pixel and coded their indices as the template feature. Xu et al. [8] proposed discriminative competitive code (DCC) and discriminative robust competitive code (DRCC), which coded the winner orientation and the ordinal relationship between its neighbors. The works mentioned above highly relied on hand-crafted filters, resulting in poor robustness and limited generalization. To address these limitations, a recent method called CompNet [31] was proposed to use competition information from deep features and demonstrated a promising performance. However, CompNet still adheres to the traditional competition mechanism and fails to consider crucial spatial information or multi-order texture features.

III. METHODOLOGY

A. Overview of the Proposed Method

Existing competition-based methods only focus on extracting the competition features along the channel dimension while ignoring spatial information and multi-order features. We propose a novel deep palmprint recognition network called CCNet to address these limitations, as depicted in Fig. 1. CCNet is composed of three branches to extract multi-scale texture features. In each branch, Gabor filter layers possess the innate ability to learn and determine the optimal hyperparameters for constructing the filters.

Once the multi-order texture features are obtained, channel and spatial competition features are extracted using the carefully designed Comp Block. Competition is exercised along both dimensions to consider channel and spatial information simultaneously. As a result, we address two crucial concerns for discriminative feature extraction - “Which is the best texture filter” and “Where the best response is located”. Moreover, the texture features of different orders are essential for different representations. The 1st-order features are more appropriate for gradual-change textures, while the 2nd-order features exhibit a satisfactory discriminative ability for mutation-change textures [21]. Therefore, we host competitions separately for 1st- and 2nd-order features to obtain rich and complementary features. By doing so, CCNet can extract comprehensive competition features, including channel, spatial, and order dimensions, and improve recognition performance.

B. Learnable Gabor Filters

Texture features are discriminative in palmprint recognition. Still, the previous works were mainly based on hand-crafted

texture filters, such as the Gaussian filter [18], Radon transform [6], and Gabor filters [32]. Among them, the Gabor filter is a popular option for palmprint texture extraction, which can effectively depict the texture orientation [3]. The Gabor filter can be expressed as:

$$G(x, y; \sigma, \gamma, u, \psi, \theta) = -e^{-\frac{\gamma^2 x'^2 + y'^2}{2(2\sqrt{2}\sigma)^2}} \cos(2\pi ux' + \psi), \quad (1)$$

where $x' = x \cos \theta + y \sin \theta$, $y' = -x \sin \theta + y \cos \theta$, and (x, y) is the coordinate index in the filter. The orientation of the Gabor filter is denoted as θ , and σ and u represent the standard deviation of the Gaussian envelope and the frequency of the sinusoidal wave, respectively. Additionally, ψ and γ are the Gaussian function's scale factor and spatial aspect ratio correspondingly.

One bottleneck of using Gabor filters for palmprint recognition is the selection of hyperparameters. In practice, different preprocessing methods or acquisition devices may cause significant heterogeneity in palmprint images, making selecting the optimal hyperparameters for the filters challenging. Therefore, a potential solution is automatically learning the relevant hyperparameters by analyzing the training data. We utilize learnable Gabor filters to optimize the hyperparameters [33]. To extract more discriminative features, CCNet utilizes different sizes of Gabor filters to extract texture features at multiple scales. Specifically, CCNet consists of three parallel texture extraction branches. The sizes of Gabor filters are set to 7×7 , 17×17 , and 35×35 for the tiny-scale, middle-scale, and large-scale branches, respectively. To leverage the benefits of multi-order features, we utilize two learnable Gabor layers to extract multi-order texture features within each texture extraction branch. This process refines the texture types and improves the discrimination of the texture features.

C. Comprehensive Competition Mechanism

Learnable Gabor filters can extract the magnitude features of the palmprint image. The basic assumption is that the Gabor magnitude response achieves its maximum if the extracted texture and filter directions coincide. The competition mechanisms typically focus on the competition results along the channel dimension. The traditional competition mechanism compares the magnitude of responses in different channels, selects the maximum response as the winner, and then takes the winner orientation index as the feature. This process aims to identify “Which texture is the best” to improve robustness and effectively handle slight dislocations between query and gallery palmprint images. Unfortunately, this method neglects spatial data and discards all other characteristics except the winner. More importantly, the conventional competitive mechanism cannot perform backpropagation, thus necessitating the manual design of the entire competitive mechanism.

To overcome the limitations of existing competition mechanisms, we propose a comprehensive competition mechanism (CCM), which considers competition along both channel and spatial dimensions. Additionally, CCM hosts a competition simultaneously in multi-order texture features, enabling more comprehensive and complementary information to be captured. Specifically, we design a Comp Block based on CCM, as illustrated in Fig. 1. To avoid missing potentially valuable features, we adopt the Soft Competition Code (SCC) for

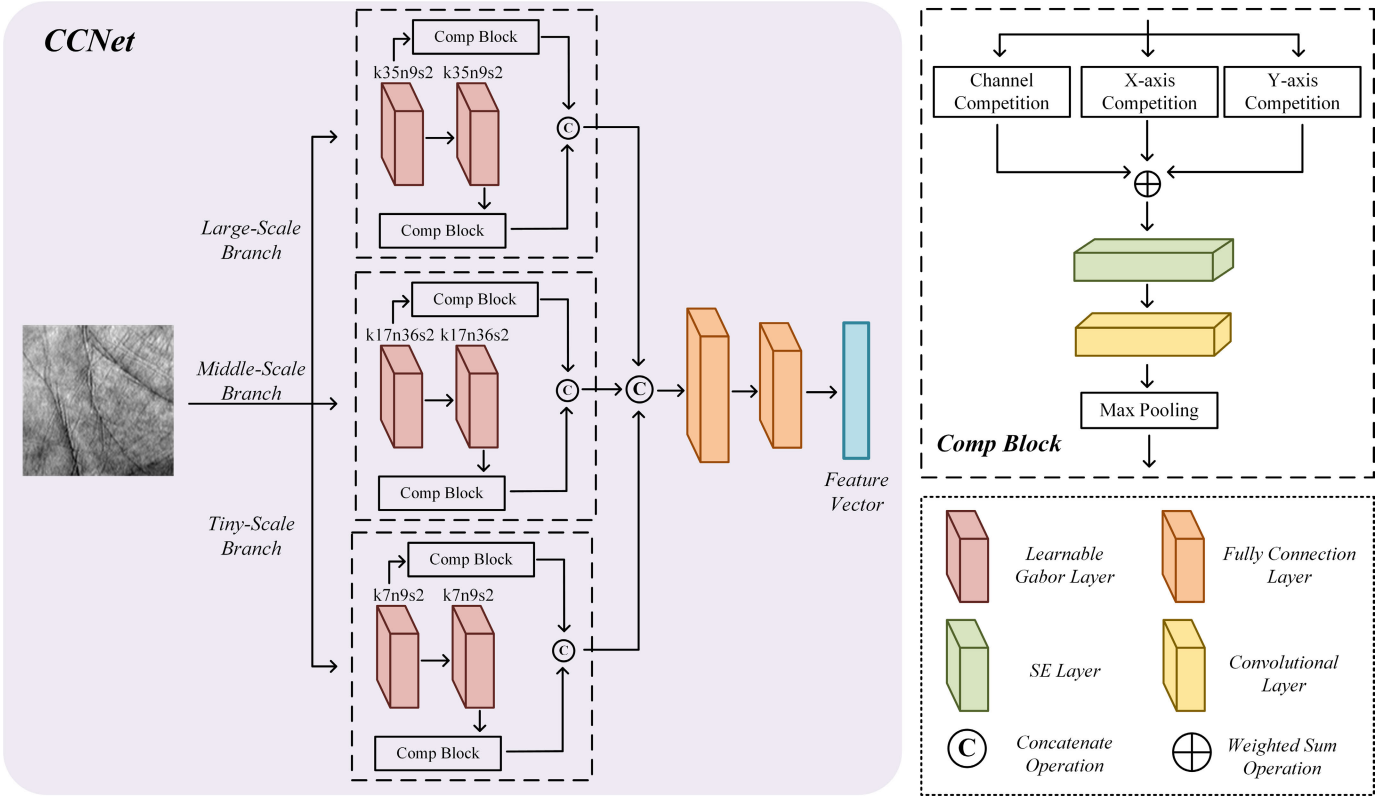


Fig. 1. The whole framework of the proposed CCNet consists of three feature extraction branches for multi-scale texture competition. Each branch contains two learnable Gabor layers. The proposed Comp Block extracts the competition features. ‘k’, ‘n’ and ‘s’ represent kernel size, number of filters, and the stride, respectively.

feature extraction [31]. SCC extracts the ordering relationship as the feature using the Softmax function, which contains more information than the winner index. The process is formulated as follows:

$$\begin{aligned} \mathbf{F}_c &= \text{Softmax}_c(\mathbf{F}_{in}), \\ \mathbf{F}_x &= \text{Softmax}_x(\mathbf{F}_{in}), \\ \mathbf{F}_y &= \text{Softmax}_y(\mathbf{F}_{in}), \end{aligned} \quad (2)$$

where $\mathbf{F}_{in} \in \mathcal{R}^{b \times c \times w \times h}$ is the input of the Comp Block, and b , c , w , h represent the batch size, channel, width, and height of the feature, respectively. $\text{Softmax}_c(\cdot)$, $\text{Softmax}_x(\cdot)$ and $\text{Softmax}_y(\cdot)$ denote the competition extraction process along channel dimension, X-axis, and Y-axis, respectively. In addition, $\mathbf{F}_c \in \mathcal{R}^{b \times c \times w \times h}$, $\mathbf{F}_x \in \mathcal{R}^{b \times c \times w \times h}$ and $\mathbf{F}_y \in \mathcal{R}^{b \times c \times w \times h}$ stand for the competition features along channel dimension, X-axis, and Y-axis, respectively.

We illustrate the process of different competition mechanisms in Fig. 2. The channel competition feature can distinguish texture orientation, while the spatial competition features (X-axis and Y-axis) can locate the best response. However, concatenating spatial competition features in a larger feature size is computationally expensive and memory-intensive. To address this issue, we designed a weighted sum operation to reduce the feature size while retaining channel and spatial competition results. The following formulation outlines this process:

$$\mathbf{F}_{out} = w_c \times \mathbf{F}_c + w_s \times (\mathbf{F}_x + \mathbf{F}_y), \quad (3)$$

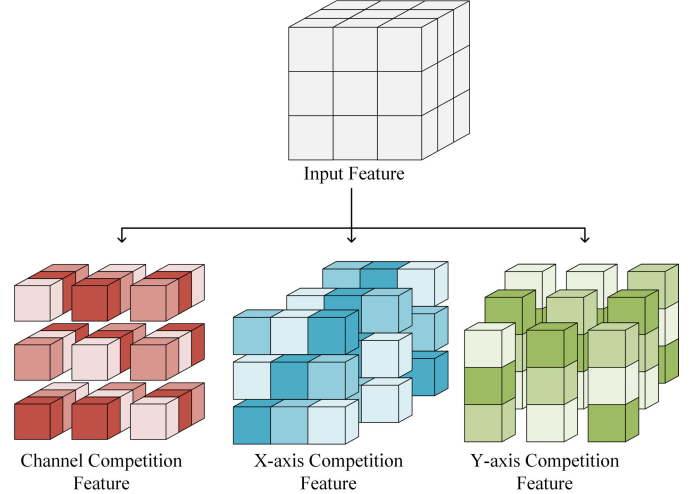


Fig. 2. A simple sample to demonstrate different competition mechanisms. Darker colors indicate better responses.

where \mathbf{F}_{out} is the output of the Comp Block, w_c and w_s denote the channel weights and two spatial competition features, respectively. They are empirically set to 0.8 and 0.1 in this paper.

After Eq. (3), a weighted feature \mathbf{F}_{out} , which contains both channel and spatial competition features, is obtained. To further enhance the discriminative power of the features, we adopt a Squeeze-and-Excitation (SE) layer [34]. The SE layer aims to determine the most useful channels by computing attention weights per channel, extracting more distinctive features. Unlike previous channel competition, the

SE layer operates on the input features containing spatial and channel competition features. CCNet incorporates a Comp Block after each learnable Gabor layer to extract multi-order texture features. This operation refines the textures and extracts more representative features, effectively capturing the competition between simultaneously-occurring features in multi-order textures. Following this, the 1st-order competition feature $\mathbf{F}_{1\text{st}}$ and the 2nd-order competition feature $\mathbf{F}_{2\text{nd}}$ are concatenated for the following feature extraction. To sum up, CCNet extracts competition features for palmprint recognition, including multi-order textures and spatial competitions through CCM. The feature is comprehensive and resilient, with various order, channel, and spatial competitions.

D. Hybrid Loss Function

In palmprint recognition networks, the model is typically optimized only using cross-entropy loss, which can be defined as:

$$\mathcal{L}_{ce} = -\frac{1}{N} \sum_{i=1}^N \sum_{c=1}^M y_{i,c} \log(p_{i,c}), \quad (4)$$

where N and M denote the numbers of samples and classes. $y_{i,c}$ and $p_{i,c}$ represent the label and the predicted probability of the i -th sample.

Unfortunately, cross-entropy loss only minimizes the distance between distinct samples and their corresponding class centers but does not effectively optimize the sample feature space. In this paper, we adopt the contrastive loss [35] to group intra-class samples and diverse inter-class samples, which is defined as:

$$\mathcal{L}_{con} = -\sum_{i \in I} \frac{1}{|P(i)|} \sum_{p \in P(i)} \log \frac{\exp(z_i \cdot z_p / \tau)}{\sum_{a \in A(i)} \exp(z_i \cdot z_a / \tau)}, \quad (5)$$

where $I = \{1 \dots 2N\}$ is the batch of contrastive sample pairs, $A(i) \equiv I \setminus \{i\}$ and i is the index of positive sample. $P(i) \equiv p \in A(i) : y_i = y_p$ is the index set of the positive samples in the batch distinct from i , and y_i is the label of the i -th sample in the batch. $|P(i)|$ is the number of samples in $P(i)$. z_a and z_p are the anchor feature and the positive features. τ is the temperature parameter. Finally, our proposed loss function is formulated as follows:

$$\mathcal{L} = w_{ce} \times \mathcal{L}_{ce} + w_{con} \times \mathcal{L}_{con}, \quad (6)$$

where w_{ce} and w_{con} are the weights of cross-entropy loss and contrastive loss, respectively, empirically set to 0.8 and 0.2 in this paper.

IV. EXPERIMENTS AND DISCUSSIONS

A. Experimental Settings and Datasets

We validated the proposed CCNet on four public palmprint recognition datasets, PolyU [4], Multi-Spectral [36], Tongji [37] and IITD [38]. Multi-Spectrum contains four sub-datasets. These datasets were collected using different ways, contact-based (PolyU), multi-spectrum-based (Multi-Spectrum), and contactless-based (Tongji and IITD) devices. By evaluating the performance of CCNet on multiple datasets, we can assess its robustness and generalizability under various

TABLE I
EERS ON DIFFERENT DATASETS (%)

	PolyU	Tongji	IITD
PalmCode	0.3500	0.1100	5.45
Ordinal Code	0.2300	0.1600	5.50
Fusion Code	0.2400	0.0731	6.20
Comp Code	0.1200	0.1100	5.50
RLOC	0.1300	0.0253	5.00
HOC	0.1600	0.0954	6.55
DOC	0.1800	0.0431	6.20
DCC	0.1500	0.0506	5.49
DRCC	0.1800	0.0308	5.42
BOCV	0.0813	0.0056	4.56
E-BOCV	0.0995	0.0180	4.65
EDM	0.0609	0.0113	4.56
2TCC	0.0834	0.0075	5.94
MTCC	0.0549	0.0043	3.94
DHN	0.0372	0.0879	4.30
DHPN	0.0320	0.0659	3.73
PalmNet	0.1110	0.0322	4.20
CompNet	0.0556	0.0250	0.54
CCNet	0.00006	0.00004	0.18

practical scenarios and demonstrate its advantages for practical palmprint recognition applications. PolyU and IITD are preprocessed under the same protocol in [39].¹

PolyU contains 7752 images from 193 individuals (386 palms). These images were collected in two sessions. There are a total of 37,800 genuine and 14,250,600 imposter matching times.

Tongji contains 12,000 images from 300 individuals (600 palms). These images were collected in two sessions, with ten images per palm and 20 images per individual. As a result, the genuine and imposter matching times are 60,000 and 35,940,000, respectively.

Multi-Spectral collected palmprint images by four different spectrum devices. This dataset contains 600 palms and can be divided into four sub-datasets, Red, Green, Blue, and Near-Infrared (NIR). Twelve images were acquired for each palm with each spectrum device. The total genuine and imposter matching times are 18,000 and 8,982,000, respectively.

IITD acquires around five images from each palm. There are a total of 2601 images. There are 1,266,840 genuine and 2,760 matching times, respectively.

To compare the performance of CCNet, we selected some classical and state-of-the-art methods, including PalmCode [4], Comp Code [5], Fusion Code [19], RLOC [6], BOCV [16], E-BOCV [17], HOC [30], DCC [8], DRCC [8], DHPN [25], PalmNet [23], EDM [20], DHN [27], 2TCC [21], MTCC [21] and CompNet [31].

To train PalmNet and DHPN, 75% of the data for each palm were used for training. For the other methods, the 1st session data were used for training; while the 2nd session data were used for testing. CCNet is implemented on the PyTorch framework and optimized by Adam [40] with a learning rate of 0.01, and the batch size is set to 512. The experimental environment used in this paper is as follows: AMD Ryzen 7 5800X CPU @3.80 GHz, 32 GB internal storage, NVIDIA GTX 3080 Ti.

¹To ensure reproducibility, we will release our training and test protocols with our codes.

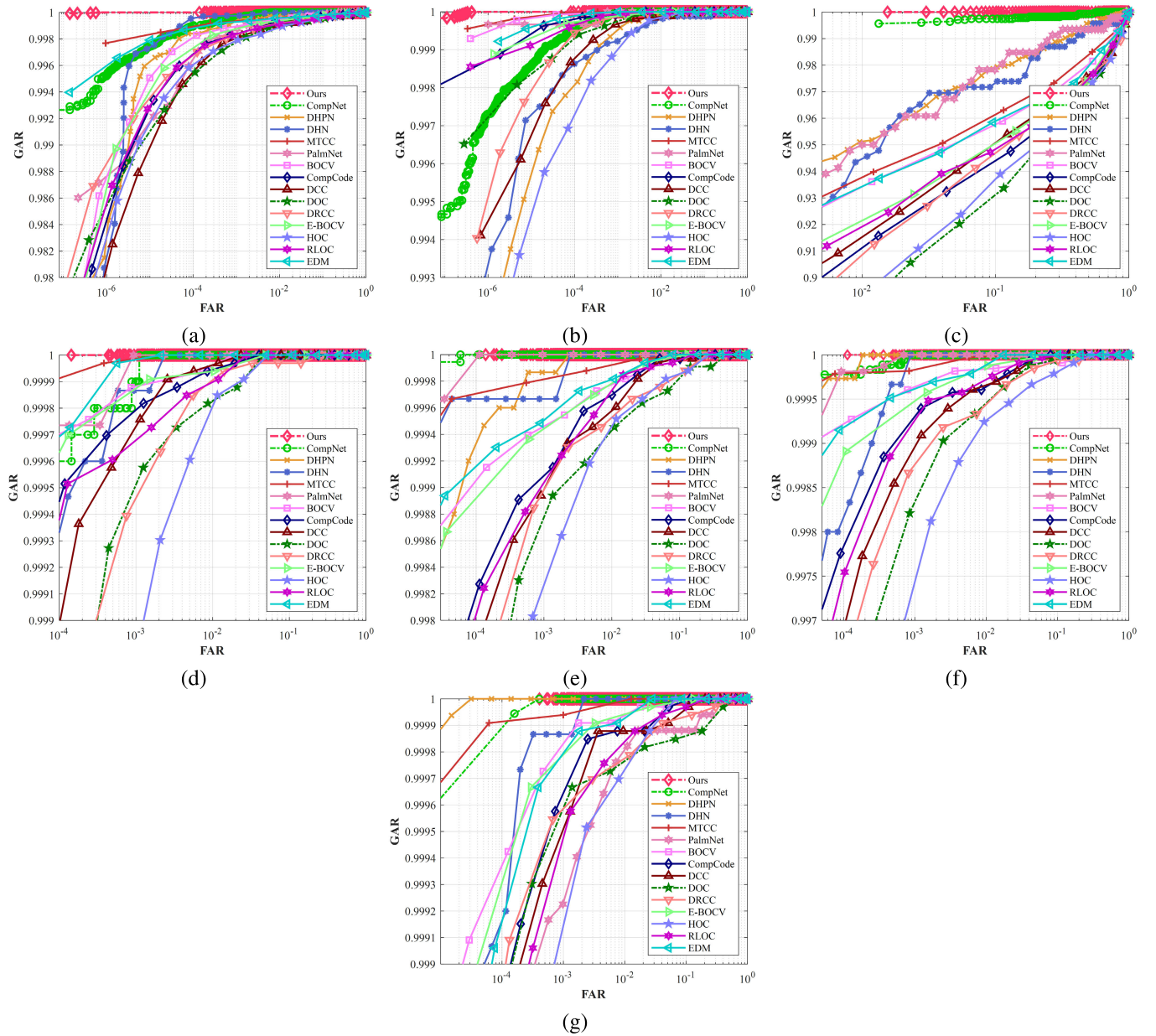


Fig. 3. The ROC curves of different methods on different datasets. (a)-(c) represent the ROC curves on PolyU, Tongji, and IITD. (d)-(g) depict the ROC curves on Red, Green, Blue, and NIR, corresponding from Multi-Spectral.

B. Experiments

Genuine Acceptance Rate (GAR) and False Accept Rate (FAR) are commonly used as validation metrics to evaluate the performance of different palmprint recognition methods. The performances of different methods were compared in terms of the Receiver Operating Characteristic (ROC) curve, which plots GAR against FAR and provides a comprehensive assessment of the trade-off between the two metrics. The better the performance is, the closer the ROC curve is to the top left corner of the plot.

The ROC curves of many typical methods are shown in Fig. 3. Our method achieved far better curves than other Tongji, IITD, and PolyU methods. In the ROC curves of IITD, CompNet, and our method, we achieved a significantly better performance than the other methods, illustrating the effectiveness of the competition mechanism for deep features.

Additionally, we would like to emphasize that our GARs are all one at the beginning of the ROC curves in all Multi-Spectrum sub-datasets, indicating that our method can perfectly distinguish between genuine and imposter samples in those sub-datasets. These results demonstrate the superior performance of our method compared with the state-of-the-art methods.

Equal Error Rate (EER) is a commonly used performance validation metric for biometric recognition methods, representing the point on the ROC where the false acceptance rate (FAR) is equal to the false rejection rate (FRR), where $FRR = 1 - GAR$. Therefore, lower EER indicates better performance. We compared the EERs of different methods on PolyU, Tongji, and IITD, respectively, and the results are shown in Tab. I. Our method achieved a far better performance than the other methods. Furthermore, our method outperforms CompNet by a significant margin. On the other hand, CompNet's performance

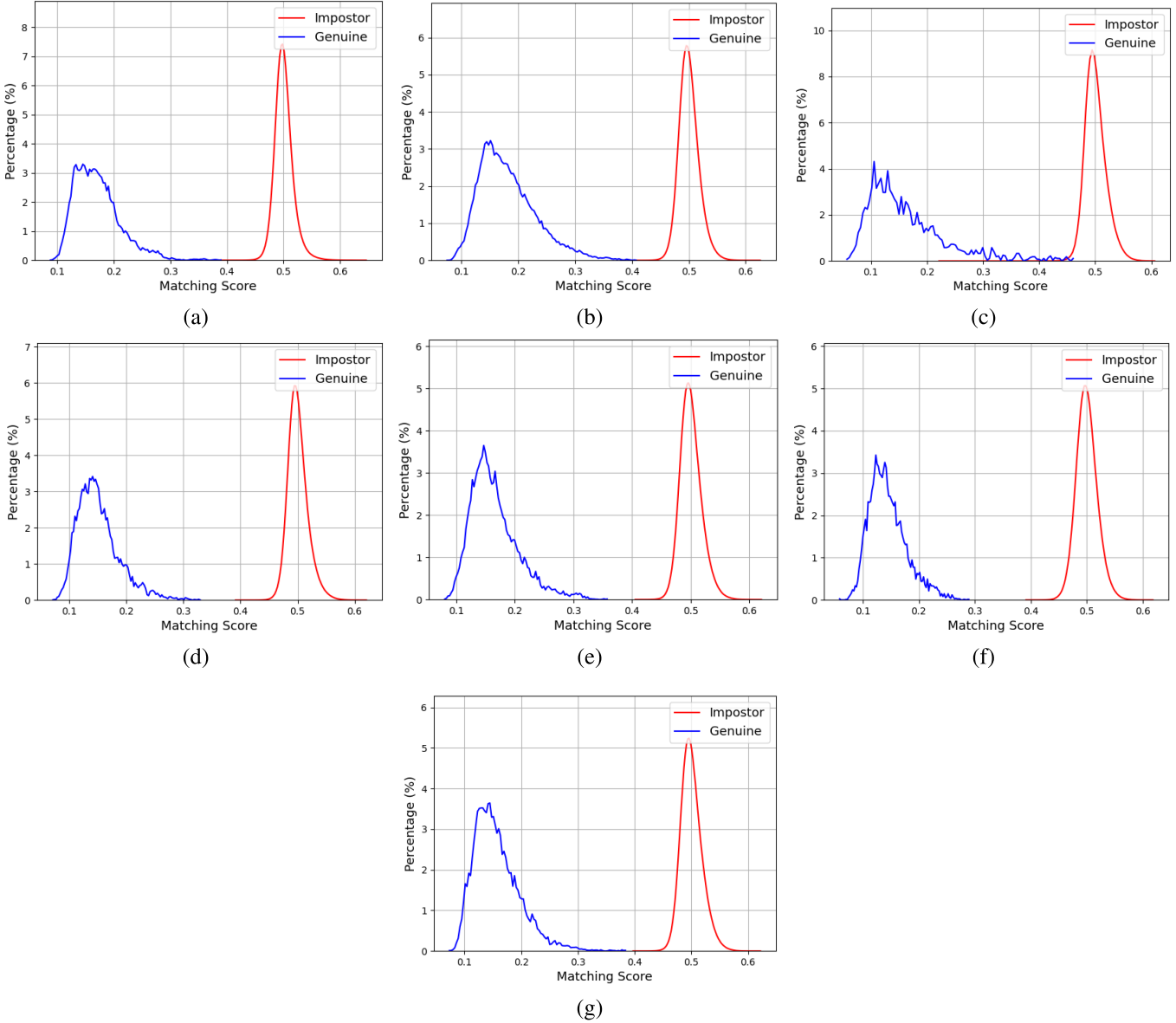


Fig. 4. Our method's genuine and imposter match distributions on different datasets. (a)-(c) depict the PolyU, Tongji, and IITD results, respectively. (d)-(g) represent results on Red, Green, Blue, and NIR, corresponding from Multi-Spectral.

is much worse than ours despite being based on the same competition mechanism. Specifically, on PolyU and Tongji, our approach outperforms CompNet by approximately 99.89% and 99.84%, respectively - a remarkable improvement over CompNet's results. Two primary factors contribute to the subpar performance of CompNet. First, it solely relies on 1st-order texture features, just like its competitors. Second, CompNet prioritizes channel information while disregarding spatial information.

Palmprint images exhibit distinct characteristics due to different acquisition wavelengths. To evaluate the robustness of CCNet across different spectra, experiments were conducted on Red, Green, Blue, and NIR spectra, and the results are shown in Table II. CCNet achieves impressive performances, 0% EERs on all sub-datasets. Like the other datasets, the two methods based on competition mechanisms achieved only satisfactory results. That being said, CompNet can achieve 0% EER in Red and fails to replicate this performance in

other datasets. However, with the proposed CCM, our method can extract more exclusive and distinctive features for palmprint recognition. This compensates for CompNet's limitations by considering channel, spatial, and multi-order competition features.

Fig. 4 shows the genuine and imposter matching distributions. Our imposter distributions are well separated from the genuine distributions, with a significant gap between the two distributions. To show the statistical discrepancy, we list the interval, average and standard deviation (STD) of both distributions in different datasets in Tab. III. It can be seen that the overlap regions between the intervals of genuine and imposter matching distributions are small in most datasets. It is worth noting that there is no overlap between the imposter and genuine samples in all spectrum sub-datasets. The results suggest that the proposed CCNet can extract discriminative features to effectively distinguish imposter samples and genuine ones. Our method boasts exceptional performance, credited to the

TABLE II
EERs ON THE MULTISPECTRAL DATASET (%)

	Red	Green	Blue	NIR
PalmCode	0.2300	0.2500	0.2800	0.2000
Ordinal Code	0.0720	0.1500	0.1600	0.1100
Fusion Code	0.1200	0.1900	0.3100	0.1700
Comp Code	0.0357	0.1100	0.0911	0.0579
RLOC	0.0444	0.0855	0.0799	0.0629
HOC	0.1000	0.1600	0.1800	0.0839
DOC	0.0584	0.1200	0.1300	0.0501
DCC	0.0450	0.0979	0.1100	0.0575
DRCC	0.0660	0.0927	0.1100	0.0563
BOCV	0.0164	0.0442	0.0358	0.0261
E-BOCV	0.0216	0.0616	0.0599	0.0315
EDM	0.0206	0.0703	0.0473	0.0363
2TCC	0.0185	0.0375	0.0405	0.0322
MTCC	0.0102	0.0213	0.0163	0.0095
DHN	0.0380	0.0304	0.0403	0.0233
DHPN	0.0369	0.0352	0.0213	0.0020
PalmNet	0.0366	0.0087	0.0178	0.0871
CompNet	0	0.0055	0.0173	0.0025
CCNet	0	0	0	0

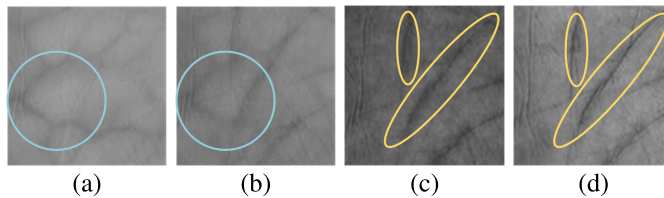


Fig. 5. Acquired samples in different spectra from the same palm. (a)-(d) represent samples in NIR, Red, Green, and Blue spectrum, respectively. The blue circles indicate veins, while the yellow circles indicate textures.

proposed CCM's outstanding discriminative feature extraction capabilities and the hybrid loss's effectiveness in optimizing the sample feature map. These factors facilitate a significant separation between the genuine and imposter distributions.

We conducted additional experiments in Multi-Spectrum to evaluate the performance of our method under different ratios of training and testing samples. The results of the verification and identification experiments are presented in Tables IV and V, respectively. CCNet achieves 0% EER in Red, Green, and Blue, except NIR. The main reason is that the palmprint textures in the NIR spectrum are not as distinctive as those in the visible spectra; some typical samples acquired by different spectra are shown in Fig. 5. Although the examples were acquired from the same palm, the captured contents differ due to the distinct physical properties of different wavelengths.

C. Ablation Study

The impact of varying weight settings in Eq. (3) is tested on the Tongji dataset. The results are shown in Fig. 6; the blue dotted line represents the baseline, only using the channel competition. The performance is effectively improved by incorporating spatial competition features. Compared to channel competition features, the spatial competition features alone do not possess remarkable discriminative ability. This implies that channel competition is a better indicator of texture type. However, since the two types of competition features complement each other, combining spatial and channel competition features can significantly enhance performance with minimal additional computational cost.

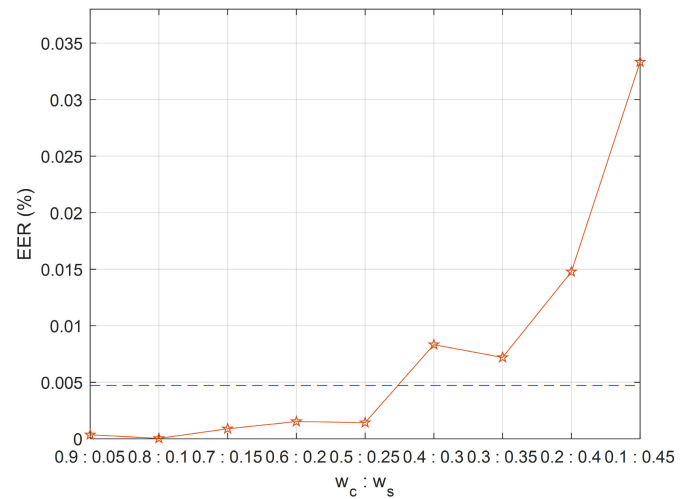


Fig. 6. The EERs under different weight settings.

The proposed CCM contains two additional competition features besides channel competition: multi-order and spatial competition. To evaluate the impact of each component, the ablation study is tested on Tongji; the results are shown in Table VI. Incorporating spatial competition can improve the performance of the 1st-order, 2nd-order, and multi-order texture features. Additionally, multi-order features are effective in enhancing performance. Therefore, spatial and multi-order competitions are crucial for enhancing the discriminative ability of palmprint recognition.

Besides that, we conducted experiments to give an ablation study for different order texture features, and the results are shown in Tab. VII. From Tab. VII, the 4th-order feature's performance has noticeably declined. This suggests that extremely high-order texture features are not helpful in accurately describing the unique characteristics of palmprint images. This could be due to high-order texture features capturing complex relationships and abstract representations within the palmprint image. Still, they may fail to capture the subtle and distinctive features necessary for identification, such as wrinkles or principal lines. Therefore, the 2nd-order texture features are suitable as high-order features for palmprint images.

D. Cross-Spectra Experiments

Our approach has been tested in a cross-spectrum scenario where palm IDs are consistent across different datasets. The CCNet is trained in the source spectra dataset and evaluated in the target spectra dataset. The identification and verification outcomes are displayed in Tables VIII and IX. Our technique shows satisfactory results in the cross-spectrum scenario, indicating strong correlations between palmprint images taken at similar wavelengths. Notably, the performance of NIR vs. Red surpasses that of NIR vs. other spectra. This indicates our method's suitability for cross-spectrum recognition.

E. Cross-ID Experiments

In this sub-section, we have tested the effectiveness of our method in both cross-ID and cross-device settings, and the results can be found in Table X. We acknowledge that

TABLE III
THE STATISTICAL INDICATORS OF GENUINE MATCHING AND IMPOSTER MATCHING DISTRIBUTIONS

	Genuine Matching		Imposter Matching	
	Interval	Average \pm STD	Interval	Average \pm STD
PolyU	[0.0880, 0.3893]	0.1708 \pm 0.0402	[0.3872, 0.6463]	0.5007 \pm 0.0163
Tongji	[0.0751, 0.4074]	0.1819 \pm 0.0499	[0.3935, 0.6256]	0.5004 \pm 0.0174
IITD	[0.0574, 0.4607]	0.1628 \pm 0.0706	[0.2214, 0.6059]	0.5005 \pm 0.0186
Red	[0.0711, 0.3291]	0.1505 \pm 0.0368	[0.3912, 0.6205]	0.5004 \pm 0.0175
Green	[0.0850, 0.3575]	0.1653 \pm 0.0412	[0.4054, 0.6206]	0.5004 \pm 0.0182
Blue	[0.0714, 0.3426]	0.1569 \pm 0.0395	[0.3923, 0.6214]	0.5003 \pm 0.0179
NIR	[0.0734, 0.3837]	0.1568 \pm 0.0407	[0.3973, 0.6218]	0.5004 \pm 0.0186

TABLE IV

EERS UNDER DIFFERENT RATIOS OF TRAINING AND TESTING SAMPLES IN MULTI-SPECTRUM

	1 : 1	1 : 2	1 : 3	1 : 5
Red	0%	0%	0%	0%
Green	0%	0%	0%	0%
Blue	0%	0%	0%	0%
NIR	0%	0%	0.00005%	0.00030%

TABLE V

ACCURACIES UNDER DIFFERENT RATIOS OF TRAINING AND TESTING SAMPLES IN MULTI-SPECTRUM

	1 : 1	1 : 2	1 : 3	1 : 5
Red	100.00%	100.00%	100.00%	100.00%
Green	100.00%	100.00%	100.00%	100.00%
Blue	100.00%	100.00%	100.00%	100.00%
NIR	100.00%	100.00%	100.00%	99.98%

TABLE VI

ABLATION RESULTS WITH DIFFERENT COMPONENTS

1st Texture	2nd Texture	Spatial Competition	EER	Accuracy
✓	✗	✗	0.00962%	100.00%
✓	✗	✓	0.00442%	99.98%
✗	✓	✗	0.03500%	99.97%
✗	✓	✓	0.03000%	99.97%
✓	✓	✗	0.00472%	100.00%
✓	✓	✓	0.00004%	100.00%

TABLE VII

ABLATION RESULTS ABOUT ORDER TEXTURE FEATURES

Texture Feature	EER	Accuracy
1st texture	0.00442%	99.98%
2nd texture	0.03000%	99.97%
3rd texture	0.04767%	99.90%
4th texture	0.09500%	99.88%
(1st+2nd) textures	0.00004%	100.00%
(1st+2nd+3rd) textures	0.00424%	100.00%
(1st+2nd+3rd+4th) texture	0.01333%	99.98%

TABLE VIII

CROSS-SPECTRA IDENTIFICATION ACCURACIES

Source	Target	Red	Green	Blue	NIR
		Red	Green	Blue	NIR
Red	/	100.00%	100.00%	100.00%	100.00%
Green	100.00%	/	100.00%	100.00%	100.00%
Blue	100.00%	100.00%	/	99.93%	
NIR	100.00%	100.00%	99.83%	/	

our cross-ID performance is not exceptional, possibly due to the network being too focused on the training set and not considering its generalization capabilities. Additionally, the loss function aims to create an optimal feature space for known IDs without any adaptation loss to enhance the network's generalization. We recognize these challenges as an exciting research field and plan to explore solutions to improve CCNet's cross-ID performance in our future works.

TABLE IX
CROSS-SPECTRA EERS

Source	Target	Red	Green	Blue	NIR
		Red	Green	Blue	NIR
Red	/	0.0278%	0.0611%	0.0091%	
Green	0.0026%	/	0%	0.2392%	
Blue	0.0130%	0%	/	0.300%	
NIR	0.0167%	0.5889%	0.6140%	/	

TABLE X

CROSS-ID PERFORMANCE

Source	Target	EER	Accuracy
Tongji	PolyU	1.57%	99.76%
IITD	PolyU	2.01%	99.63%
PolyU	Tongji	2.22%	98.48%
IITD	Tongji	3.22%	98.35%

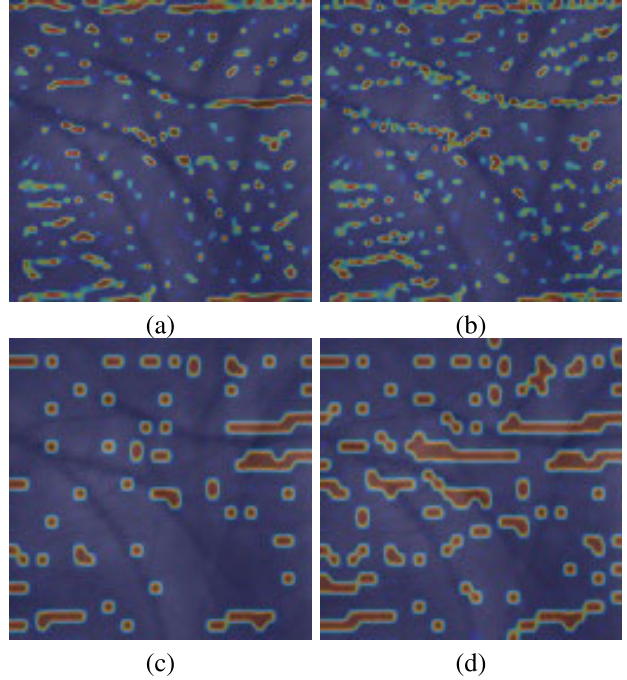


Fig. 7. The competition heatmaps. (a)-(b) represent the low-order competition heatmaps of traditional competition mechanisms and CCM, respectively. (c)-(d) represent the high-order competition heatmaps of traditional competition mechanisms and CCM, respectively.

F. Visualization

In this sub-section, we compared the traditional competition mechanism and our CCM and visualized their competition heatmaps in Fig. 7. It is evident that the areas of interest in the traditional low-order and high-order competition heatmaps are pretty limited. However, CCM has proven to expand the focused regions significantly. Besides that, it is apparent

that lower-level competition characteristics effectively depict the gradual shift in textures, particularly the principal lines. Meanwhile, the high-order features exhibit a satisfactory discriminative ability for mutation change. Hence, low-order and high-order competition features are complementary. This way, CCM can help the network learn more discriminative features by combining channel, spatial, and order dimensions information.

V. CONCLUSION

In this paper, we reconsidered the traditional competition mechanism and introduced a novel comprehensive competition mechanism (CCM). Furthermore, a novel palmprint recognition network called CCNet is proposed to utilize CCM and achieve remarkable performances on four public palmprint datasets. Our study demonstrates that spatial and multi-order competition features, which were previously overlooked, are significant for palmprint recognition. Our CCM is both efficient and effective, requiring minimal computational resources. This study highlights the importance of comprehensive competition features.

While CCNet has demonstrated impressive capabilities, the results of its cross-ID functionality may not be in line with anticipated standards. As a result, a possible topic in our future work is to adaptively balance the tradeoff between the accuracy for the known palms and the robustness for the unknown palms. Most palmprint recognition methods assume that data can be transferred to the server for centralized learning. This operation carries a risk of releasing private information in palmprint images. Based on this consideration, exploring how to combine palmprint recognition with the privacy-preserving distributed learning paradigm is an interesting topic.

REFERENCES

- [1] Q. Zhu, Y. Zhou, L. Fei, D. Zhang, and D. Zhang, "Multi-spectral palmprints joint attack and defense with adversarial examples learning," *IEEE Trans. Inf. Forensics Security*, vol. 18, pp. 1789–1799, 2023.
- [2] H. Shao and D. Zhong, "Learning with partners to improve the multi-source cross-dataset palmprint recognition," *IEEE Trans. Inf. Forensics Security*, vol. 16, pp. 5182–5194, 2021.
- [3] L. Fei, G. Lu, W. Jia, S. Teng, and D. Zhang, "Feature extraction methods for palmprint recognition: A survey and evaluation," *IEEE Trans. Syst., Man, Cybern., Syst.*, vol. 49, no. 2, pp. 346–363, Feb. 2019.
- [4] D. Zhang, W.-K. Kong, J. You, and M. Wong, "Online palmprint identification," *IEEE Trans. Pattern Anal. Mach. Intell.*, vol. 25, no. 9, pp. 1041–1050, Sep. 2003.
- [5] A. W.-K. Kong and D. Zhang, "Competitive coding scheme for palmprint verification," in *Proc. 17th Int. Conf. Pattern Recognit.*, 2004, pp. 520–523.
- [6] W. Jia, D.-S. Huang, and D. Zhang, "Palmprint verification based on robust line orientation code," *Pattern Recognit.*, vol. 41, no. 5, pp. 1504–1513, May 2008.
- [7] L. Fei, Y. Xu, W. Tang, and D. Zhang, "Double-orientation code and nonlinear matching scheme for palmprint recognition," *Pattern Recognit.*, vol. 49, pp. 89–101, Jan. 2016.
- [8] Y. Xu, L. Fei, J. Wen, and D. Zhang, "Discriminative and robust competitive code for palmprint recognition," *IEEE Trans. Syst., Man, Cybern., Syst.*, vol. 48, no. 2, pp. 232–241, Feb. 2018.
- [9] L. Fei, W. K. Wong, S. Zhao, J. Wen, J. Zhu, and Y. Xu, "Learning spectrum-invariance representation for cross-spectral palmprint recognition," *IEEE Trans. Syst., Man, Cybern., Syst.*, vol. 53, no. 6, pp. 3868–3879, Jun. 2023.
- [10] A. Iula and D. Nardiello, "3-D ultrasound palmprint recognition system based on principal lines extracted at several under skin depths," *IEEE Trans. Instrum. Meas.*, vol. 68, no. 12, pp. 4653–4662, Dec. 2019.
- [11] D. Zhong, H. Shao, and X. Du, "A hand-based multi-biometrics via deep hashing network and biometric graph matching," *IEEE Trans. Inf. Forensics Security*, vol. 14, no. 12, pp. 3140–3150, Dec. 2019.
- [12] D. Zhong, X. Du, and K. Zhong, "Decade progress of palmprint recognition: A brief survey," *Neurocomputing*, vol. 328, pp. 16–28, Feb. 2019.
- [13] S. Zhang, H. Wang, W. Huang, and C. Zhang, "Combining modified LBP and weighted SRC for palmprint recognition," *Signal, Image Video Process.*, vol. 12, no. 6, pp. 1035–1042, Sep. 2018.
- [14] L. Fei, B. Zhang, Y. Xu, C. Tian, I. Rida, and D. Zhang, "Jointly heterogeneous palmprint discriminant feature learning," *IEEE Trans. Neural Netw. Learn. Syst.*, vol. 33, no. 9, pp. 4979–4990, Sep. 2022.
- [15] L. Fei, B. Zhang, W. Jia, J. Wen, and D. Zhang, "Feature extraction for 3-D palmprint recognition: A survey," *IEEE Trans. Instrum. Meas.*, vol. 69, no. 3, pp. 645–656, Mar. 2020.
- [16] Z. Guo, D. Zhang, L. Zhang, and W. Zuo, "Palmprint verification using binary orientation co-occurrence vector," *Pattern Recognit. Lett.*, vol. 30, no. 13, pp. 1219–1227, Oct. 2009.
- [17] L. Zhang, H. Li, and J. Niu, "Fragile bits in palmprint recognition," *IEEE Signal Process. Lett.*, vol. 19, no. 10, pp. 663–666, Oct. 2012.
- [18] Z. Sun, T. Tan, Y. Wang, and S. Z. Li, "Ordinal palmprint representation for personal identification," in *Proc. IEEE/CVF Int. Conf. Comput. Vis. Pattern Recognit. (CVPR)*, vol. 1, 2005, pp. 279–284.
- [19] A. Kong, D. Zhang, and M. Kamel, "Palmprint identification using feature-level fusion," *Pattern Recognit.*, vol. 39, no. 3, pp. 478–487, Mar. 2006.
- [20] Z. Yang, L. Leng, and W. Min, "Extreme downsampling and joint feature for coding-based palmprint recognition," *IEEE Trans. Instrum. Meas.*, vol. 70, pp. 1–12, 2021.
- [21] Z. Yang, L. Leng, T. Wu, M. Li, and J. Chu, "Multi-order texture features for palmprint recognition," *Artif. Intell. Rev.*, vol. 56, no. 2, pp. 995–1011, Feb. 2023.
- [22] T. Chai, S. Prasad, and S. Wang, "Boosting palmprint identification with gender information using DeepNet," *Future Gener. Comput. Syst.*, vol. 99, pp. 41–53, Oct. 2019.
- [23] A. Genovese, V. Piuri, K. N. Plataniotis, and F. Scotti, "PalmNet: Gabor-PCA convolutional networks for touchless palmprint recognition," *IEEE Trans. Inf. Forensics Security*, vol. 14, no. 12, pp. 3160–3174, Dec. 2019.
- [24] D. Zhong and J. Zhu, "Centralized large margin cosine loss for open-set deep palmprint recognition," *IEEE Trans. Circuits Syst. Video Technol.*, vol. 30, no. 6, pp. 1559–1568, Jun. 2020.
- [25] D. Zhong, S. Liu, W. Wang, and X. Du, "Palm vein recognition with deep hashing network," in *Proc. Chin. Conf. Pattern Recognit. Comput. Vis. (PRCV)*, 2018, pp. 38–49.
- [26] H. Zhu, M. Long, J. Wang, and Y. Cao, "Deep hashing network for efficient similarity retrieval," in *Proc. AAAI Conf. Artif. Intell. (AAAI)*, vol. 30, no. 1, 2016, pp. 1–7.
- [27] T. Wu, L. Leng, M. K. Khan, and F. A. Khan, "Palmprint-palmvein fusion recognition based on deep hashing network," *IEEE Access*, vol. 9, pp. 135816–135827, 2021.
- [28] X. Dong, S. Cho, Y. Kim, S. Kim, and A. B. J. Teoh, "Deep rank hashing network for cancellable face identification," *Pattern Recognit.*, vol. 131, Nov. 2022, Art. no. 108886.
- [29] X. Dong, M. K. Khan, L. Leng, and A. B. J. Teoh, "Co-learning to hash palm biometrics for flexible IoT deployment," *IEEE Internet Things J.*, vol. 9, no. 23, pp. 23786–23794, Dec. 2022.
- [30] L. Fei, Y. Xu, and D. Zhang, "Half-orientation extraction of palmprint features," *Pattern Recognit. Lett.*, vol. 69, pp. 35–41, Jan. 2016.
- [31] X. Liang, J. Yang, G. Lu, and D. Zhang, "CompNet: Competitive neural network for palmprint recognition using learnable Gabor kernels," *IEEE Signal Process. Lett.*, vol. 28, pp. 1739–1743, 2021.
- [32] X. Liang, Z. Li, D. Fan, J. Li, W. Jia, and D. Zhang, "Touchless palmprint recognition based on 3D Gabor template and block feature refinement," *Knowl.-Based Syst.*, vol. 249, Aug. 2022, Art. no. 108855.
- [33] P. Chen, W. Li, L. Sun, X. Ning, L. Yu, and L. Zhang, "LGCN: Learnable Gabor convolution network for human gender recognition in the wild," *IEICE Trans. Inf. Syst.*, vol. 102, no. 10, pp. 2067–2071, 2019.
- [34] J. Hu, L. Shen, S. Albanie, G. Sun, and E. Wu, "Squeeze-and-excitation networks," *IEEE Trans. Pattern Anal. Mach. Intell.*, vol. 42, no. 8, pp. 2011–2023, Aug. 2020.
- [35] P. Khosla et al., "Supervised contrastive learning," *Adv. Neural Inf. Process. Syst.*, vol. 33, pp. 18661–18673, 2020.
- [36] D. Zhang, Z. Guo, G. Lu, L. Zhang, and W. Zuo, "An online system of multispectral palmprint verification," *IEEE Trans. Instrum. Meas.*, vol. 59, no. 2, pp. 480–490, Feb. 2010.

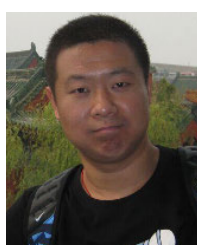
- [37] L. Zhang, L. Li, A. Yang, Y. Shen, and M. Yang, "Towards contactless palmprint recognition: A novel device, a new benchmark, and a collaborative representation based identification approach," *Pattern Recognit.*, vol. 69, pp. 199–212, Sep. 2017.
- [38] A. Kumar and S. Shekhar, "Personal identification using multibiometrics rank-level fusion," *IEEE Trans. Syst., Man, Cybern., C Appl. Rev.*, vol. 41, no. 5, pp. 743–752, Sep. 2011.
- [39] T. Wu, L. Leng, and M. K. Khan, "A multi-spectral palmprint fuzzy commitment based on deep hashing code with discriminative bit selection," *Artif. Intell. Rev.*, vol. 56, pp. 6169–6186, Nov. 2022.
- [40] D. P. Kingma and J. Ba, "Adam: A method for stochastic optimization," 2014, *arXiv:1412.6980*.



Ziyuan Yang received the M.S. degree in computer science from the School of Information Engineering, Nanchang University, Nanchang, China, in 2021. He is currently pursuing the Ph.D. degree with the College of Computer Science, Sichuan University, Chengdu, China. His research interests include biometrics, distributed learning, and security analysis.



Huijie Huangfu received the B.S. degree from the College of Computer Science, Sichuan University, Chengdu, China, in 2021, where he is currently pursuing the M.S. degree. His research interests include computer vision and deep learning.



Lu Leng (Member, IEEE) received the Ph.D. degree from Southwest Jiaotong University, Chengdu, China, in 2012. He performed the post-doctoral research with Yonsei University, Seoul, South Korea, and the Nanjing University of Aeronautics and Astronautics, Nanjing, China. He was a Visiting Scholar with West Virginia University, USA, and Yonsei University. Currently, he is a Full Professor with Nanchang Hangkong University. He has granted several scholarships and funding projects in his academic research. He has published more than 100 international journal and conference papers. His research interests include computer vision, biometric template protection, and biometric recognition. He is a member of the Association for Computing Machinery (ACM), the China Society of Image and Graphics (CSIG), and the China Computer Federation (CCF). He is a reviewer of several international journals and conferences.



Bob Zhang (Senior Member, IEEE) received the B.A. degree in computer science from York University, Toronto, ON, Canada, in 2006, the M.A.Sc. degree in information systems security from Concordia University, Montreal, QC, Canada, in 2007, and the Ph.D. degree in electrical and computer engineering from the University of Waterloo, Waterloo, ON, in 2011. After graduating from the University of Waterloo, he was with the Center for Pattern Recognition and Machine Intelligence. Later, he was a Post-Doctoral Researcher with the Department of Electrical and Computer Engineering, Carnegie Mellon University, Pittsburgh, PA, USA. He is currently an Associate Professor with the Department of Computer and Information Science, University of Macau, Macau. His research interests focus on biometrics, pattern recognition, and image processing. He is a Technical Committee Member of the IEEE Systems, Man, and Cybernetics Society. He is an Associate Editor of IEEE TRANSACTIONS ON NEURAL NETWORKS AND LEARNING SYSTEMS, *Artificial Intelligence Review*, and *IET Computer Vision*.



Andrew Beng Jin Teoh (Senior Member, IEEE) received the B.Eng. and Ph.D. degrees in electronics from the National University of Malaysia, in 1999 and 2003, respectively. He is a Full Professor with the Electrical and Electronic Engineering Department, College of Engineering, Yonsei University, South Korea. He has received funding for his research, focuses on biometric applications and biometric security. He has published over 350 international refereed journal articles and conference papers and has edited several book chapters and book volumes. His current research interests are machine learning and information security. He served as a Guest Editor for *IEEE Signal Processing Magazine*; and an Associate Editor for IEEE TRANSACTIONS ON INFORMATION FORENSIC AND SECURITY, IEEE BIOMETRICS COMPENDIUM, and *Machine Learning with Applications* (Elsevier).



Yi Zhang (Senior Member, IEEE) received the B.S., M.S., and Ph.D. degrees in computer science and technology from the College of Computer Science, Sichuan University, Chengdu, China, in 2005, 2008, and 2012, respectively. From 2014 to 2015, he was with the Department of Biomedical Engineering, Rensselaer Polytechnic Institute, Troy, NY, USA, as a Post-Doctoral Researcher. He is currently a Full Professor with the School of Cyber Science and Engineering, Sichuan University, and the Director of the Deep Imaging Group (DIG). He has authored more than 80 papers in the field of image processing. These papers were published in several leading journals, including IEEE TRANSACTIONS ON MEDICAL IMAGING, IEEE TRANSACTIONS ON COMPUTATIONAL IMAGING, *Medical Image Analysis*, *European Radiology*, and *Optics Express* and reported by the Institute of Physics (IOP) and during the Lindau Nobel Laureate Meeting. He received major funding from the National Key Research and Development Program of China, the National Natural Science Foundation of China, and the Science and Technology Support Project of Sichuan Province, China. His research interests include medical imaging, compressive sensing, and deep learning. He is a Guest Editor of the *International Journal of Biomedical Imaging and Sensing and Imaging* and an Associate Editor of IEEE TRANSACTIONS ON MEDICAL IMAGING and IEEE TRANSACTIONS ON RADIATION AND PLASMA MEDICAL SCIENCES.